

Unique Double Carbon Protection Structured Co_3O_4 Anode for Lithium Ion Battery

Dawei Luo¹, Yuban Lei², Ning Zhao¹, Hang He¹, Khan Abrar¹, Kun Li^{1*}

¹School of Applied Chemistry and Biological Technology, Shenzhen Polytechnic, Shenzhen, China

²Department of Resource Engineering, Guangxi Modern polytechnic college, Hechi, China

Email: *likun@szpt.edu.cn

How to cite this paper: Luo, D.W., Lei, Y.B., Zhao, N., He, H., Abrar, K. and Li, K. (2020) Unique Double Carbon Protection Structured Co_3O_4 Anode for Lithium Ion Battery. *Journal of Materials Science and Chemical Engineering*, 8, 56-70.
<https://doi.org/10.4236/msce.2020.812005>

Received: November 11, 2020

Accepted: December 21, 2020

Published: December 24, 2020

Copyright © 2020 by author(s) and Scientific Research Publishing Inc. This work is licensed under the Creative Commons Attribution International License (CC BY 4.0).

<http://creativecommons.org/licenses/by/4.0/>



Open Access

Abstract

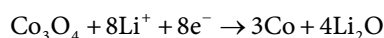
In this study, novel Carbon aerogel (CA)/ Co_3O_4 /Carbon (C) composites with a double protective structure are synthesized through a solvothermal method and in-situ polymerization. The morphology and structure are characterized by X-ray diffraction, scanning electron microscopy (SEM), high-resolution transmission electron microscopy (HRTEM), and Fourier transform infrared spectroscopy (FTIR). The loading content of active anode material Co_3O_4 in the composite is investigated by thermogravimetry, and the electrochemical properties of the composite are characterized by electrochemical impedance spectroscopy (EIS). The SEM results show that the nano-sized spherical Co_3O_4 particle is adhered to the inner Carbon aerogel (CA). The HRTEM result indicates the thickness of the prepared Carbon (C) up to 40 nm. Nano-sheet is coated on the surface of the Co_3O_4 particle. Compared with the pure Co_3O_4 anode materials, the Carbon aerogel (CA)/ Co_3O_4 /Carbon (C) composites have better transport kinetics for both electron and lithium-ion in EIS testing results, which may contribute to its higher specific capacity and higher first coulomb efficiency. Due to the unique structure of the composite material with double protection against the volume expansion of Co_3O_4 when charged, the Carbon aerogel (CA)/ Co_3O_4 /Carbon (C) composite material exhibits better cycle stability with a discharge capacity of 1180 mAh/g after 50 cycles. Therefore, the double protection strategy is verified as an effective method to improve the electrochemical performance of transition metal oxide with carbon composite as an anode material in lithium battery.

Keywords

Carbon Protection, Co_3O_4 Anode, Lithium Ion Battery

1. Introduction

Due to the relatively high energy density and outstanding electrochemical performance, the rechargeable Li-ion battery has become the mainstream power source in the electrical vehicle (EV), the electrical storage system (ESS), and consumer electronic products (CE) in recent years [1] [2] [3]. For commercialized lithium battery, the anode material of graphite has a relatively low theoretical specific capacity of 372 mAh/g, which cannot meet the increasing demands of energy density for lithium batteries. Recently, a lot of research has been devoted to the electrochemical active transition metal oxides (TMOs) as promising anode materials (SnO₂ [4], TiO₂ [5], ZnO [6], Fe₃O₄ [7] and α -Fe₂O₃ [8], Co₃O₄ [9]-[19]), due to their high theoretical capacities (>700 mAh/g) and abundance in nature. Among these TMOs, Co₃O₄ is one of the most promising candidates, which owns a large theoretical capacity (about 890 mAh/g) and remarkable electrochemical properties [9]-[19]. Before commercializing the transition metal oxides anode materials, at least three obstacles need to be overcome. The first one is the massive volume expansion when the lithium-ion is charging, combined with the insertion of the Li-ion into the anode material crystal structure, resulting in the electrode pulverization with fast reversible capacity fading during cycling. The other is the poor ionic and electronic conductivity of the TMOs, leading to the high AC and DC resistance of the battery and the low discharge capacity under the large discharge current. The electrochemical reaction below occurs for Co₃O₄ nanoparticles during the initial charging process, which formed the Li₂O with the loss of reversible lithium ions:



Owing to the irreversible reaction between the lithium-ion and Co₃O₄, the low 1st-coulomb efficiency is a crucial factor which hinders its commercialization.

Up to now, the composites of transition metal oxides with carbon materials, such as graphene [20], carbon nanotube [21], carbon fibers [22], and carbon aerogel [23] [24] has attracted more and more researchers' attention. It is suggested that these carbon materials have a relatively large surface area, good electronic conductivity, and mechanical flexibility, which could increase the kinetics of the electrochemical reaction and inhibit the pulverization of the electrode material. [8]

Co₃O₄/carbonaceous composite anode materials exhibit the improvement of electrochemical performance compared with the pure Co₃O₄ particles. These composites include the Co₃O₄/acetylene black composites [25], the Co₃O₄/carbon aerogel composites [23] [24], and Co₃O₄/graphene composites [26] [27]. The common feature of all the composites above is just modified from one dimension, to stabilize material structure from both inner and outside; we introduce the carbon coating layer on the Carbon aerogel (CA)/Co₃O₄ composite. In this article, we have reported a composite material Carbon aerogel (CA)/Co₃O₄/Carbon (C), which consists of the macroporous architecture of three-dimensional carbon aerogel (CA) with the nano-sized spherical Co₃O₄ particle, and the nano-thickness carbon layer. This structure is designed as a double protection structure, aiming to pro-

protect the Co_3O_4 from exposure of the electrolyte and alleviate the pulverization of anode materials from both the inner and outside. Compared with pure Co_3O_4 particles, this double protection Carbon Aerogel (CA)/ Co_3O_4 /Carbon (C) composites exhibit improved electrochemical performance, including the higher specific capacity, electrochemical kinetic and cycling stability.

2. Experiment

2.1. Material and Chemicals

All the chemical reagents were analytical grade. Carbon aerogel (CA) was synthesized through a typical Sol-gel method [28]. $\text{Co}(\text{NO}_3)_2 \cdot 6\text{H}_2\text{O}$, octanol, anhydrous alcohol, sodium dodecyl sulfate were obtained from Sinopharm Chemical Reagent Cooperation (Beijing China).

A three-step process preparation of the Carbon aerogel (CA)/ Co_3O_4 /Carbon (C) composite has been applied, which includes the synthesis of Carbon aerogel (CA) by supercritical drying firstly, then the loading of active material nano-sized Co_3O_4 particles on CA by solvothermal method in octanol solution, and the coating of polypyrrole by in-situ chemical polymerization and the final carbonation under high temperature.

The 0.05 g Carbon aerogel was dispersed into 50 mL octanol by ultrasonic dispersion for 1 h treatment, after that, 0.5 g $\text{Co}(\text{NO}_3)_2 \cdot 6\text{H}_2\text{O}$ was added in to the solution. After stirring for 15 min, the solution was heated at 180°C for 16 h in a Teflon-lined stainless-steel autoclave. The hydrothermal reaction products were washed with distilled water for 3 times, and then dried at 60°C under vacuum conditions for 12 h. Finally, the pure Carbon aerogel (CA)/ Co_3O_4 composite powder was obtained.

The Carbon aerogel (CA)/ Co_3O_4 /Carbon (C) composite was synthesized through an in-situ chemical polymerization. The Carbon aerogel (CA)/ Co_3O_4 composite powder was dispersed in 100 mL deionized water. After adding 10 mL sodium dodecyl sulfate, the solution was stirred for 4 h for a homogenous dispersion. Then, the 50 μL pyrrole monomer and 0.2 g $\text{FeCl}_3 \cdot 6\text{H}_2\text{O}$ were added and the mixture was stirred for 4 h at room temperature. The as-obtained Carbon aerogel (CA)/ Co_3O_4 /PPy composite precipitates were washed several times with deionized water and then dried at 80°C under vacuum for 6 h.

The obtained Carbon aerogel (CA)/ Co_3O_4 /PPy composite was heat-treated under N_2 atmosphere at 450°C for 45 min and then cooled to room temperature. Finally, the composite of Carbon aerogel (CA)/ Co_3O_4 /Carbon (C) was obtained.

For comparison, the pure Co_3O_4 was fabricated in the absence of Carbon aerogel (CA) and Carbon (C) under the same condition.

2.2. Material Characterization

The crystal structure information of these samples were characterized by X-ray diffractometer (XRD, Rigaku D/MAX-2550) with $\text{CuK}\alpha$ radiation in the 2θ range of $10^\circ - 80^\circ$, and Fourier transform infrared spectroscopy (FTIR, MAGNAIR750)

in the wave-numbered range of 1000 - 4000 cm^{-1} . The morphology of these samples were characterized by a (FESEM, SEM, HITACHI, SU-70) and a (TEM, JEOL 2100F) at an acceleration voltage of 200 kV. The mass content loading of the active materials Co_3O_4 was characterized by the thermogravimetric (TG) analysis under airflow at a rate of $10^\circ\text{C min}^{-1}$ in the range of $30^\circ\text{C} - 900^\circ\text{C}$. The specific surface area (BET) of the composite's material was evaluated by N_2 adsorption/desorption isotherm at 77K (V-sorb 2800TP), and the pore size distribution was determined by the adsorption branch of isotherms based on the Barrett-Joyner-Halenda (BJH) model.

2.3. Electrochemical Measurement

The electrochemical properties of the composites were evaluated using the CR2032-type coin cells assembled in a dry argon-filled glove box. The working electrodes were prepared by mixing 80 wt% of the active composite Carbon aerogel (CA)/ Co_3O_4 /Carbon (C), 10 wt% conductive carbon black (Super-P), and 10 wt% poly (vinylidene fluoride) binder dissolved in *N*-methyl-pyrrolidinone (NMP) solvent. The active material slurry was coated on the Cu foil with a slot die. After coating and drying, the active material electrode was cut into small discs with a diameter of 12 mm. The Li metal foil with the diameter of 16 mm was used as the counter electrode, and the Celgard 2400 PP separator with the diameter of 18 mm was used as separator. The electrolyte was obtained by dissolving $1 \text{ mol}\cdot\text{L}^{-1}$ LiPF_6 in ethylene carbonate (EC) and dimethyl carbonate (DMC) (1:1 v/v) [29].

The galvanostatic charge/discharge and cycling performance were tested by a CT2001A Land battery system at room temperature in the voltage range of 0.01 - 3.0 V. The galvanostatic charge/discharge tests were measured at a scan rate of 0.1C, and the cycling performance as tested at a scan rate of 0.5C. The electrochemical impedance spectroscopy (EIS) measurement were tested in the frequency range from 0.01 Hz to 100 kHz, using a CHI660E (Shanghai Chenhua, China) electrochemical workstation.

3. Results and Discussion

3.1. Structural Characterization Results

Figure 1 shows the XRD patterns of the bare Co_3O_4 and Carbon aerogel (CA)/ Co_3O_4 /Carbon (C) composites samples. The (111), (200), (311), (400), (422), (511), and (440) peaks in the XRD patterns indicates the face-centered cubic Co_3O_4 (fcc, $Fd\bar{3}m$, JCPDS No.42-1467). Compared with the Co_3O_4 , the pattern of Carbon aerogel (CA)/ Co_3O_4 /Carbon (C) is inclined to the baseline, which indicates that the Carbon aerogel (CA)/ Co_3O_4 is coated by amorphous carbon. Also, the broader peak of the Carbon aerogel (CA)/ Co_3O_4 /Carbon (C) composite suggests the smaller crystal size of the Co_3O_4 . No other diffraction peaks appear, indicating the amorphous carbon coating does not change the crystal structure of Co_3O_4 .

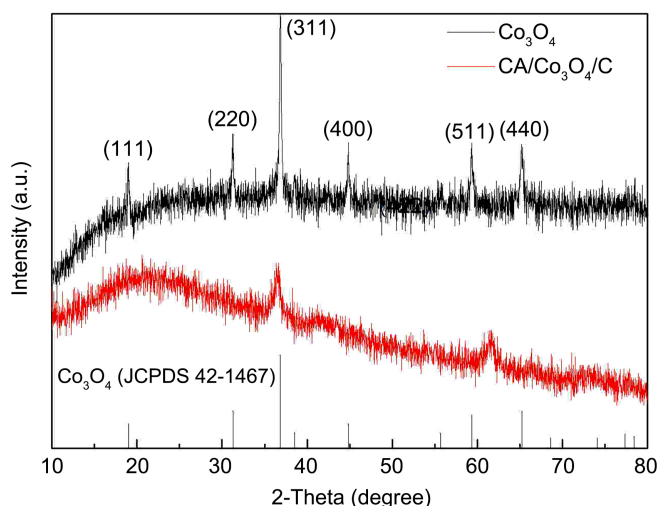


Figure 1. XRD pattern of the Co_3O_4 and CA/ Co_3O_4 /C composite.

The morphology and micro-structure of Carbon aerogel (CA)/ Co_3O_4 /Carbon (C) composites were observed through SEM and HR-TEM, as shown in **Figure 2**. The pure Co_3O_4 particles have spherical morphology with a diameter about 800 nm - 1500 nm, some particles are adhering to each other as shown in **Figure 2(a)**. Due to high specific surface area of Carbon aerogel (CA) and its 3D network structure composed of interconnected carbon spheres, the Co_3O_4 nanoparticles are adsorbed on Carbon's surface aerogel (CA), and the distribution of Co_3O_4 is uniform and random. As shown in **Figure 2(c)** and **Figure 2(d)**, the morphology of the Carbon aerogel (CA)/ Co_3O_4 /PPy and Carbon aerogel (CA)/ Co_3O_4 /Carbon (C) composites varies a little, suggesting that the coating layer is thin and do not change the structure and morphology of the composite of Carbon aerogel (CA)/ Co_3O_4 . Further investigation of HR-TEM reveals that the carbon layer with the thickness of 40 nm is equally coated on the surface of Co_3O_4 as shown in **Figure 2(e)**, demonstrating the nanoparticles of Co_3O_4 are well protected from the erosion of the electrolyte by the carbon layer, which is also acting as the buffer layer inhibiting the pulverization of the anode electrode when charging and discharging repeatedly. As show in **Figure 2(f)**, the lattice image from the CA/ Co_3O_4 /PPy could be clearly seen in the high resolution TEM (HRTEM) lattice image. The lattice spacing is about 0.24 nm, which could be assigned to (113) inter planar of the crystal structure for Co_3O_4 .

To further study the structure of carbon coating on the composite of Carbon aerogel (CA)/ Co_3O_4 /Carbon (C). The Fourier transform infrared spectroscopy (FTIR, MAGNAIR750) in the wave-numbered range of 1000 - 4000 cm^{-1} was tested for both Carbon aerogel (CA)/ Co_3O_4 /Carbon (C) composites and the pure Co_3O_4 . As shown in **Figure 3**, compared with the pure Co_3O_4 , no prominent new peaks were observed for the composite of Carbon aerogel (CA)/ Co_3O_4 /Carbon (C), which indicates the polypyrrole (PPy) was fully carbonized. The broad and strong peak at 3404 cm^{-1} may attributed to the O-H stretching vibration, and the peaks at 2927 cm^{-1} can be assigned to the vibration mode of -CH group [8] [30].

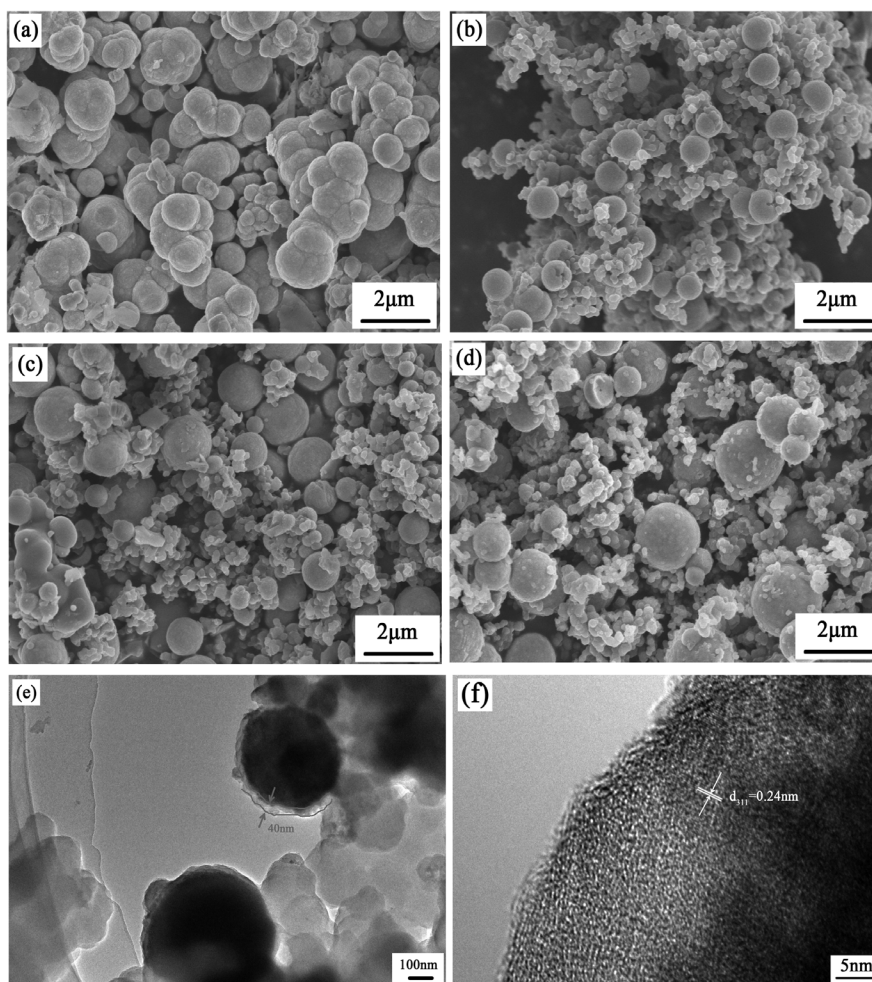


Figure 2. SEM images of (a) Co_3O_4 , and (b) (c) (d) $\text{CA}/\text{Co}_3\text{O}_4/\text{C}$ composite at different magnifications, high-resolution TEM images (e) and (f) of $\text{CA}/\text{Co}_3\text{O}_4/\text{C}$ composite.

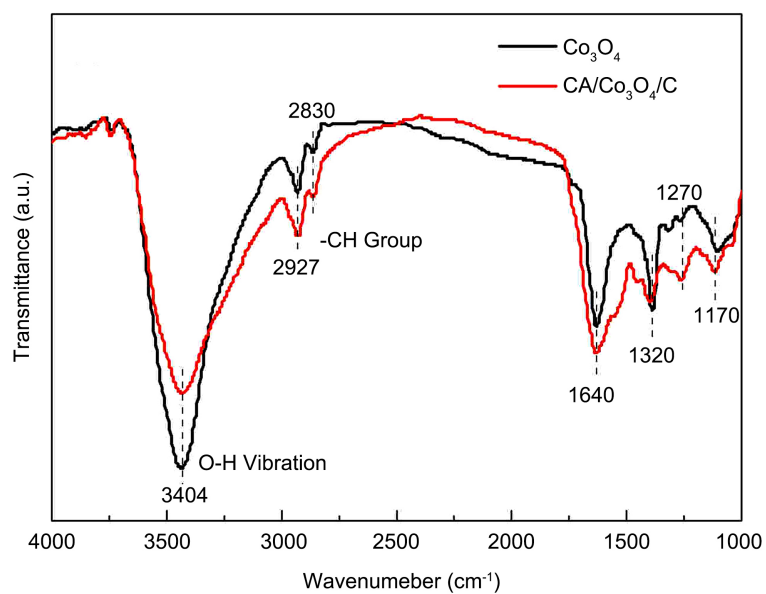


Figure 3. FTIR of the Co_3O_4 and $\text{CA}/\text{Co}_3\text{O}_4/\text{C}$ composite.

To investigate the mass content of the Co_3O_4 in the composites of Carbon aerogel (CA)/ Co_3O_4 /Carbon (C), the thermogravimetric analysis (TGA) was conducted in the air from RT to 900°C . As shown in **Figure 4**, the weight loss of ~ 2 wt% below 250°C could be ascribed to removing the water adsorbed on the surface. The weight loss of ~ 44.9 wt% between 250°C and 700°C could be ascribed to the combustion of Carbon aerogel (CA) and Carbon (C) in the air. The results could be deduced that the amount of active material Co_3O_4 in the composites of Carbon aerogel (CA)/ Co_3O_4 /Carbon (C) is about 53.1%.

The specific surface area (BET) of the composites material was measured to further investigate the porous structure of the composite. As shown in **Figure 5**, the test result exhibits a hysteresis loop in the adsorption/desorption curve, indicating the existence of well-developed porous structure. The specific surface area (BET) of the Carbon aerogel (CA) is $219.25\text{ m}^2/\text{g}$, indicating the excellent characteristic for loading Co_3O_4 active material. After loading the active material of Co_3O_4 nanoparticles and the carbon coating, the specific surface area (BET) of Carbon aerogel (CA)/ Co_3O_4 /Carbon (C) composite decrease to $10.8\text{ m}^2/\text{g}$. The pore structure of Carbon aerogel (CA)/ Co_3O_4 /Carbon (C) composite was further verified by the Barrett-Joyner-Halendathe (BJH) calculation in the inset of **Figure 5**. The average size of the pores is about 5 nm, indicating the abundant mesopores in the composite structure. These pores could improve the electrolyte's infiltration in the cathode and anode electrode and improve electrochemical reaction activity; the unique porous structure could also relieve the inner stress generation by the volume changes of the Co_3O_4 during the lithiation-delithiation process.

3.2. Electrochemical Characterization Results

A standard method based on Carbon aerogel (CA)/ Co_3O_4 /Carbon (C) composite—Li half cell was used to evaluate the electric-chemical performance. **Figure 6**

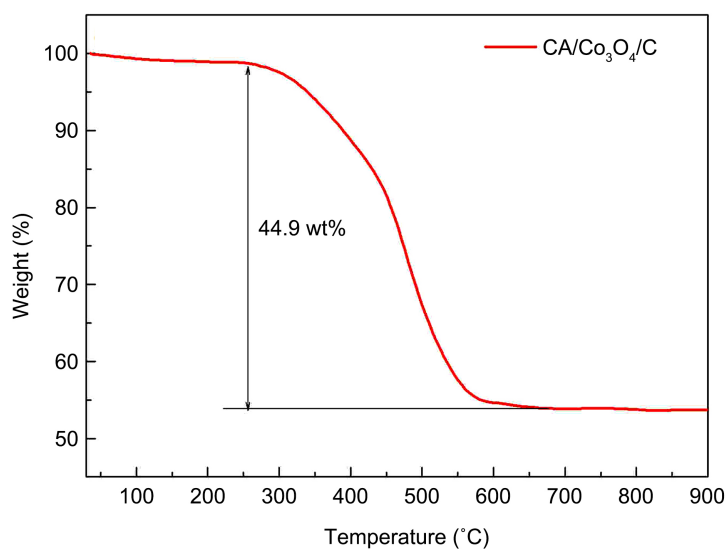


Figure 4. Thermal gravity result of the CA/ Co_3O_4 /C composite.

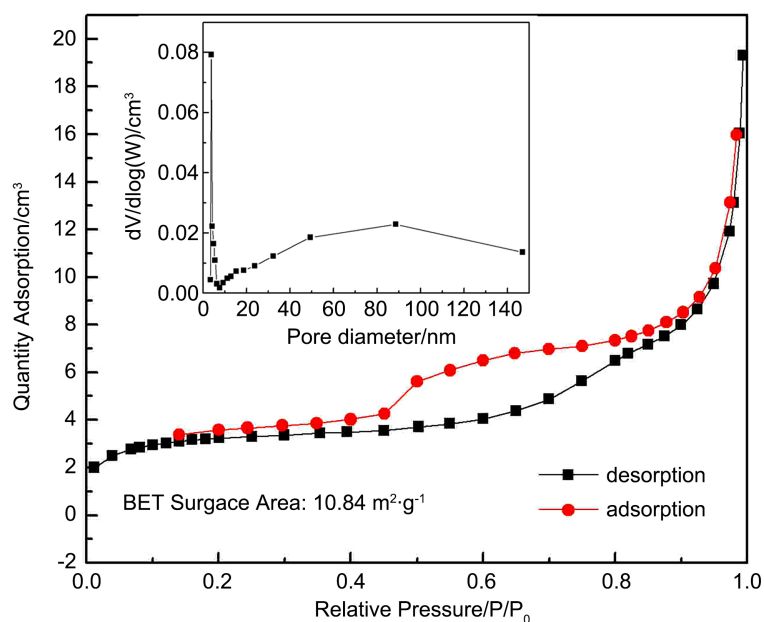


Figure 5. Nitrogen adsorption isotherms of the CA/Co₃O₄/C composite.

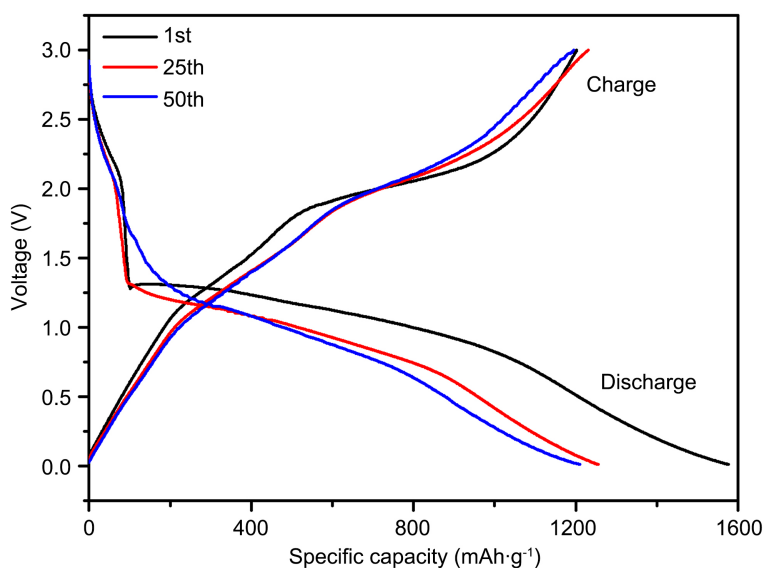


Figure 6. Galvanostatic charge and discharge profile of the CA/Co₃O₄/C composite.

shows the galvanostatic charge/discharge profile at a constant current rate of 100 mA·g⁻¹ in the 1st, 25th and 50th charge-discharge curves, respectively. The first discharge specific capacity of the composite is about 1600 mAh/g. The first charge specific capacity is about 1280 mAh/g, which is much higher than both the theoretical specific capacity of Co₃O₄ and Carbon aerogel's theoretical prediction value (CA)/Co₃O₄/Carbon (C) composite. This phenomenon has been observed in many transition oxide composites, and the underlying mechanism is still under debate [31] [32] [33]. Some of the researches ascribe it to the formation of a solid electrolyte interface (SEI) layer, which can store the interfacial Li

ions [23], some ascribe it to the identical porous structure of CA, which can provide host-sites for the reduction of lithium ions [32], the recent study indicates the spin-polarized electrons can be stored in the already-reduced metallic nano-particles and contributes to the charge surface capacity [33]. The first discharge curve exhibits a platform between 0.9 V to 1.1 V, followed by a declining curve to a discharge cutoff voltage, which is the typical character for the pure Co_3O_4 material [34]. In the 50th charge-discharge curve, the voltage platform slightly decreases, indicating the increase of the Ohmic and electrochemical resistance after cycling.

Figure 7(a) shows the cycling performance of the Carbon aerogel (CA)/ Co_3O_4 /Carbon (C) electrode and pure Co_3O_4 particle at a constant current rate of $100 \text{ mA}\cdot\text{g}^{-1}$ up to 50 cys at room temperature. The discharge capacity of pure Co_3O_4 decreased to 380 mAh/g with the capacity retention of 63.3% at the 50th cycle. While for the Carbon aerogel (CA)/ Co_3O_4 /Carbon (C) composite, the capacity retention is about 88.3% at the 50th cycle, much higher than the pure Co_3O_4 particle. This phenomenon indicates that the porous CA structure and the carbon coating benefit the structure stability of the Co_3O_4 anode materials with high cycling performance. The Coulomb efficiency of 98.5% could be achieved after 50 discharge/charge cycles in Carbon aerogel (CA)/ Co_3O_4 /Carbon (C) composite, higher than the pure Co_3O_4 particle of 94.8%, suggesting that more reversible oxidation-reduction reaction with less losing of Li-ion in cycling for composite. Like many other transition metal oxides, for pure Co_3O_4 , the huge volume swelling and destruction of the structure may result in SEI formation and losing reversible Li ion repeating in each charge/discharge cycle. For Carbon aerogel (CA)/ Co_3O_4 /Carbon (C) composite, the carbon coating and porous CA structure could improve the electrode electronic conductivity and relieve the volume swelling, improving the quality of the carbon the cycling performance [8].

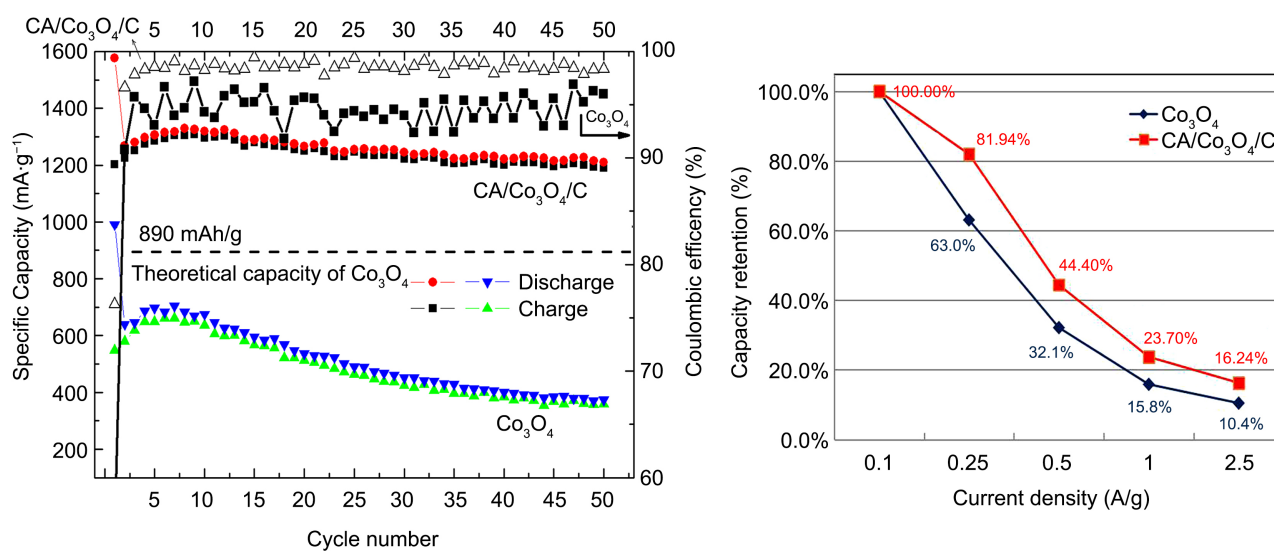


Figure 7. Cycling performance and rate capability performance of the Co_3O_4 and CA/ Co_3O_4 /C composite.

As shown in **Figure 7(b)**, the rate performances of the composite electrode compare with are evaluated at different current density from 0.1C to 2.5C. When the current density is 0.1 A/g, the discharge capacity is 1080 mAh/g for the Carbon aerogel (CA)/Co₃O₄/Carbon (C) composite, and 780 mAh/g for the pure Co₃O₄. When the current density increases to 0.25 A/g, 0.5 A/g, 1 A/g, 2.5 A/g, the ratio of discharge capacity to that at 0.1 A/g is 81.94%, 44.4%, 23.7% and 16.24% for the Carbon aerogel (CA)/Co₃O₄/Carbon (C) composite, higher than that of 63%, 32.1%, 15.7% and 10.4% for the pure Co₃O₄. The better rate performance for the composite of Carbon aerogel (CA)/Co₃O₄/Carbon (C) indicates the unique double protection strategy for the composite of Carbon aerogel (CA)/Co₃O₄/Carbon (C) may improve its electronic conductivity and the electrochemical reaction kinetic. Some reported Co₃O₄-based nanostructures in the last two years are listed in **Table 1**. By contrast, the cycling performance of Carbon aerogel (CA)/Co₃O₄/Carbon (C) is higher than those of Co₃O₄ nanocage/Co₃O₄ nanoframework/TiO₂ [12], Co₃O₄ nanocubes [13], Hollow Co-Co₃O₄/CNTs [14], Co₃O₄/nitrogen-doped carbon composite [15] and Co₃O₄ nanocomposite [19]. But, it is admirable that Co₃O₄/nitrogen-doped carbon composite in reference [16], Co/Co₃O₄ nanoparticles in reference [17] and porous Mn-Co₃O₄/C microspheres in reference [18] show super cyclability and rate capability. Nevertheless, the cycling stability and rate capability of Carbon aerogel (CA)/Co₃O₄/Carbon (C) composite anode are also superior to most of previous reports, indicating that the Carbon aerogel (CA)/Co₃O₄/Carbon (C) composite obtained in this study is a promising anode materials for LIBs.

Table 1. Specific capacities of Co₃O₄-based nanostructures in the literature.

Samples	Current density/mA·g ⁻¹	Discharge capacity (N th)/mAh·g ⁻¹	References and published year
Co ₃ O ₄ nanocage/Co ₃ O ₄ nanoframework/TiO ₂	200	~600 (50)*	[12], 2019
Co ₃ O ₄ nanocubes	100	873.5 (50)	[13], 2019
Hollow Co-Co ₃ O ₄ /CNTs	200	806.7 (200)	[14], 2019
Co ₃ O ₄ -doped hollow hierarchical porous carbon spheres	200	1291.7 (200)	[15], 2019
Co ₃ O ₄ /nitrogen-doped carbon composite	100	423 (100)	[16], 2019
Co/Co ₃ O ₄ nanoparticles	200	1823 (200)	[17], 2020
Porous Mn-Co ₃ O ₄ /C microspheres	1000	901 (300)	[18], 2020
Co ₃ O ₄ nanocomposite	1000	428 (50)	[19], 2020
Carbonaerogel (CA)/Co ₃ O ₄ /Carbon (C) composite	100	1180 (50)*	This work

To further compare and study the electrode reaction kinetics of the Carbon aerogel (CA)/Co₃O₄/Carbon (C) composite and the pure Co₃O₄ active materials, electrochemical impedance spectroscopy (EIS) performance was tested. The impedance spectra were collected by applying an 5 mV AC voltage perturbation over the frequency from 0.1 Hz to 100 kHz, and the result could provide detail information of each component of resistance by different reaction process, including the resistance of the electrolyte, solid electrolyte interface (SEI), charge transfer, and Li⁺ diffusion in the electrode [35] [36] [37]. As presented in **Figure 8**, for both samples, depressed semicircles are observed in the middle frequency range in the Nyquist plots, which is often considered as the response of charge transfer resistance (R_{ct}) between the electrolyte and the electrode. The charge transfer resistance is well fitted by an equivalent circuit model as shown in the inset of **Figure 8**, the fitting results of the R_{ct} values are 350.2Ω and 275.7Ω for Co₃O₄ and the (CA)/Co₃O₄/Carbon (C) composites electrode, respectively, indicating the increasing of electrochemically active sites and kinetic after introducing the CA and Carbon coating layer on the Co₃O₄ particles. The fitting result of the R_s value is 4.16Ω for the (CA)/Co₃O₄/Carbon (C) composites electrode, which is smaller than 7.81Ω of the pure Co₃O₄. This phenomenon indicates that the carbon coating could improve electronic conductivity and reduce the Ohmic impedance. The EIS and equivalent circuit model fitting results display that the double protective structure could effectively facilitate both the electronic conductivity and electrochemical kinetic of the active material of Co₃O₄.

To investigate the structural stability of the Carbon aerogel (CA)/Co₃O₄/Carbon (C) composites during the charging and discharging process, the composite electrode after cycled 50 circles was carefully cleaned and observed using SEM. As shown in **Figure 9**, the microstructure of the Co₃O₄ particles varies little compared to the fresh electrode, no serious damage or agglomeration of the Co₃O₄ nanoparticles is observed, indicating the high structure stability when

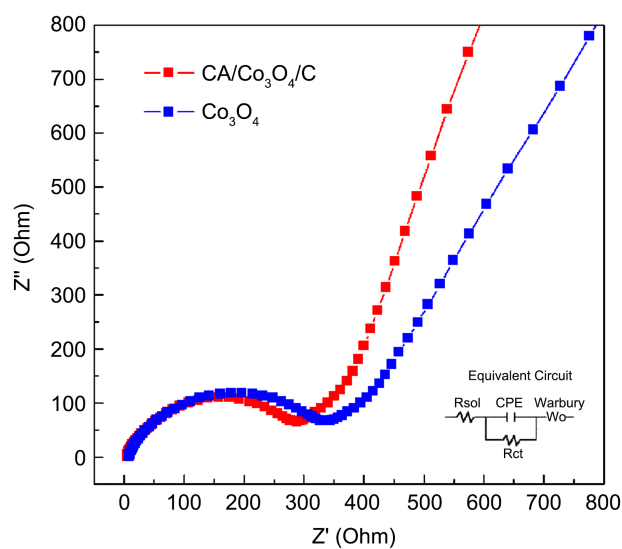


Figure 8. Nyquist plots of the Co₃O₄ and CA/Co₃O₄/C composite.

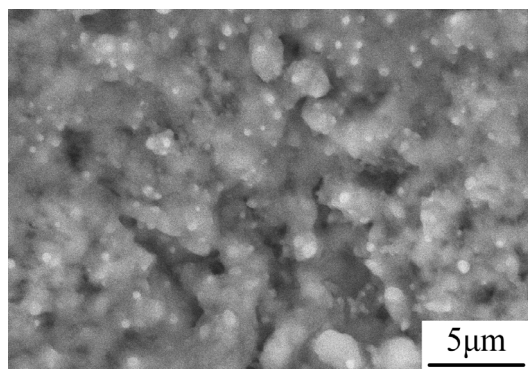


Figure 9. SEM image of CA/Co₃O₄/C composite after 50 cycle.

charge and discharge repeatedly. Similar results have been reported in other transition metal anode materials (TMOs) like Fe₃O₄ [8], indicating the supportive effect of the carbonaceous materials on the structure of TMO anode materials. The excellent structure stability may attribute to the unique double protective structure of Carbon aerogel (CA)/Co₃O₄/Carbon (C) composites as follows: The Carbon aerogels played an important role in supporting and loading the active materials of Co₃O₄ nonparticles with its identical porous skeleton structure; the nano thickness outer layer of carbon adhering to the Co₃O₄ surface firmly, which could relieve the volume expansion and agglomeration when charging.

4. Conclusion

In this work, a double protection Carbon aerogel (CA)/Co₃O₄/Carbon (C) composites have been successfully synthesized by a simple solvothermal method combined with subsequent in-situ polymerization of polypyrrole (PPy) composite and then heat-treatment under N₂ atmosphere. The composite with 53.1% loading of Co₃O₄ possessed a specific discharge capacity of 1280 mAh/g in the first cycle, higher than both the theoretical specific capacity of Co₃O₄ (890 mAh/g). The cycle and rate performance were determined with excellent cycle stability and high-rate capability. The further in the investigation of the electrode after cycling indicates the more stable structural stability. The unique structure with inner Carbon aerogel and outer Carbon coating layer provides double protection against the swelling and crack of the nano-particles and provides double protection against the swelling and crack of the nano-particles and enhances the electronic conductivity and electrochemical kinetic. These results suggest that the Carbon aerogel (CA)/Co₃O₄/Carbon (C) composite is a very promising candidate for high energy density anode materials of the next-generation LIBs.

Acknowledgements

This work is supported by the Nature Science Foundation of Guangdong Province (2018A030313371), Youth Innovative Talent Project of Guangdong Province College (2017GkQNCX061) and Innovation project of Shenzhen Polytech-

nic (CXGC2020C0009).

Conflicts of Interest

The authors declare no conflicts of interest regarding the publication of this paper.

References

- [1] Lecce, D.D., Verrelli, R. and Hassoun, J. (2017) Lithium-Ion Batteries for Sustainable Energy Storage: Recent Advances towards New Cell Configurations. *Green Chemistry*, **19**, 3442-3467. <https://doi.org/10.1039/C7GC01328K>
- [2] Lu, Y., Zhang, Q. and Chen, J. (2019) Recent Progress on Lithium-Ion Batteries with high Electrochemical Performance. *Science China Chemistry*, **62**, 533-548. <https://doi.org/10.1007/s11426-018-9410-0>
- [3] Liu, Y.Y., Zhou, G.M., Liu, K. and Cui, Y. (2017) Design of Complex Nanomaterials for Energy Storage: Past Success and Future Opportunity. *Accounts of Chemical Research*, **50**, 2895-2905. <https://doi.org/10.1021/acs.accounts.7b00450>
- [4] Heo, J., Haridas, A.K., Li, X.Y., Saroha, R., Lee, Y., Lim, D.H., Cho, K.K. and Ahn, J.H. (2020) Controlling the Voltage Window for Improved Cycling Performance of SnO₂ as Anode Material for Lithium-Ion Batteries. *Journal of Nanoscience and Nanotechnology*, **20**, 7051-7056. <https://doi.org/10.1166/jnn.2020.18834>
- [5] Zhang, Y.Y., Tang, Y.X., Li, W.L. and Chen, X.D. (2016) Nanostructured TiO₂-Based Anode Materials for High-Performance Rechargeable Lithium-Ion Batteries, *ChemNanoMat*, **8**, 764-775. <https://doi.org/10.1002/cnma.201600093>
- [6] Wang, L., Zhang, G.H., Liu, Q.H. and Duan, H.G. (2018) Recent Progress in Zn-Based Anodes for Advanced Lithium Ion Batteries. *Materials Chemistry Frontiers*, **2**, 1414-1435. <https://doi.org/10.1039/C8QM00125A>
- [7] Jiang, Y., Jiang, Z.J., Yang, L.F., Cheng, S. and Liu, M.L. (2015) A High-Performance Anode for Lithium Ion Batteries: Fe₃O₄ Microspheres Encapsulated in Hollow Graphene Shells. *Journal of Materials Chemistry A*, **3**, 11847-11856. <https://doi.org/10.1039/C5TA01848J>
- [8] Luo, D.W., Liu, S.S., Lin, F., Yu, L.H. and Zhang, J.J. (2018) Fabrication and Characterization of Double Protective Carbon Aerogel (CA)/Alpha-Fe₂O₃@Polypyrrole (PPy) Composites as an Anode Material for High Performance Lithium Ion Batteries. *Solid State Ionics*, **321**, 1-7. <https://doi.org/10.1016/j.ssi.2018.03.027>
- [9] Kong, L.L., Wang, L., Sun, D.Y., Meng, S., Zu, D.D., He, Z.X., Dong, X.Y., Li, Y.F. and Jin, Y.C. (2019) Aggregation-Morphology-Dependent Electrochemical Performance of Co₃O₄ Anode Materials for Lithium-Ion Batteries. *Molecules*, **24**, 3149. <https://doi.org/10.3390/molecules24173149>
- [10] Fu, Y.J., Li, X.W., Sun, X.L., Wang, X.H., Liu, D.Q. and He, D.Y. (2012) Self-Supporting Co₃O₄ with Lemongrass-Like Morphology as a High-Performance Anode Material for Lithium Ion Batteries. *Journal of Materials Chemistry*, **22**, 17429-17431. <https://doi.org/10.1039/c2jm33704e>
- [11] Donders, M.E., Knoops, H.C.M., Kessels, W.M.M. and Notten, P.H.L. (2012) Co₃O₄ as Anode Material for Thin Film Micro-Batteries Prepared by Remote Plasma Atomic Layer Deposition. *Journal of Power Sources*, **203**, 72-77. <https://doi.org/10.1016/j.jpowsour.2011.12.020>
- [12] Wang, L., Yuan, Y.F., Zheng, Y.Q., Zhang, X.T., Yin, S.M. and Guo, S.Y. (2019) Cap-

- sule-Like Co_3O_4 Nanocage/ Co_3O_4 Nanoframework/ TiO_2 Nodes as Anode Material for Lithium-Ion Batteries. *Materials Letters*, **253**, 5-8.
<https://doi.org/10.1016/j.matlet.2019.06.021>
- [13] Liu, Y.G., Wan, H.C., Jiang, N., *et al.* (2019) Chemical Reduction-Induced Oxygen Deficiency in Co_3O_4 Nanocubes as Advanced Anodes for Lithium Ion Batteries. *Solid State Ionics*, **334**, 117-124. <https://doi.org/10.1016/j.ssi.2019.02.014>
- [14] Li, Y.F., Fu, Y.Y., Liu, W.B., Song, Y.H. and Wang, L. (2019) Hollow $\text{Co-Co}_3\text{O}_4/\text{CNTs}$ Derived from ZIF-67 for Lithium Ion Batteries. *Journal of Alloys and Compounds*, **784**, 439-446. <https://doi.org/10.1016/j.jallcom.2019.01.085>
- [15] Yu, M.K., Sun, Y.X., Du, H.R., *et al.* (2019) Hollow Porous Carbon Spheres Doped with a Low Content of Co_3O_4 as Anode Materials for High Performance Lithium-Ion Batteries. *Electrochimica Acta*, **317**, 562-569.
<https://doi.org/10.1016/j.electacta.2019.06.027>
- [16] Qiu, J.H., Yu, M., Zhang, Z.H., Cai, X. and Guo, G.H. (2019) Synthesis of $\text{Co}_3\text{O}_4/\text{Nitrogen-Doped Carbon Composite}$ from Metal-Organic Framework as Anode for Li-Ion Battery. *Journal of Alloys and Compounds*, **775**, 366-371.
<https://doi.org/10.1016/j.jallcom.2018.10.129>
- [17] Zhang, C.W., Song, Y., Xu, L.B. and Yin, F.X. (2020) *In Situ* Encapsulation of $\text{Co}/\text{Co}_3\text{O}_4$ Nanoparticles in Nitrogen-Doped Hierarchically Ordered Porous Carbon as High Performance Anode for Lithium-Ion Batteries. *Chemical Engineering Journal*, **380**, 122545. <https://doi.org/10.1016/j.cej.2019.122545>
- [18] Zhang, K.B., Guo, P.Y., Zeng, M., Zhang, Y.Q., Bai, Y. and Li, J. (2020) Double Modification to Effectively Improve Electrochemical Performance of Co_3O_4 as Li-Ion Batteries Anode. *Materials Letters*, **280**, Article ID: 128558.
<https://doi.org/10.1016/j.matlet.2020.128558>
- [19] Keshmarzi, M.K., Zonouz, A.F., Poursalehi, F., *et al.* (2020) Electrophoretic Deposition of Nanographitic Flakes/ Co_3O_4 Nanocomposite Layers Synthesized by Solvothermal Process for Improved Lithium-Ion-Battery Anode. *Journal of Solid State Chemistry*, **288**, Article ID: 121471. <https://doi.org/10.1016/j.jssc.2020.121471>
- [20] Tan, Q.K., Kong, Z., Chen, X.J., Zhang, L., Hu, X.Q., Mu, M.X., Sun, H.C., Shao, X.C., Guan, X.G., Gao, M. and Xu, B.H. (2019) Synthesis of $\text{SnO}_2/\text{Graphene Composite}$ Anode Materials for Lithium-Ion Batteries. *Applied Surface Science*, **485**, 314-322.
<https://doi.org/10.1016/j.apsusc.2019.04.225>
- [21] Xu, M.W., Wang, F., Zhang, Y., Yang, S., Zhao, M.S. and Song, X.P. (2013) Co_3O_4 -Carbon Nanotube Heterostructures with Bead-on-String Architecture for Enhanced Lithium Storage Performance. *Nanoscale*, **5**, 8067-8072.
<https://doi.org/10.1039/c3nr02538a>
- [22] Zhang, C.L., Lu, B.R., Cao, F.H., Yu, Z.L., Cong, H.P. and Yu, S.H. (2018) Hierarchically Structured $\text{Co}_3\text{O}_4/\text{carbon Porous Fibers}$ Derived from Electrospun ZIF-67/PAN Nanofibers as Anodes for Lithium Ion Batteries. *Journal of Materials Chemistry A*, **6**, 12962-12968. <https://doi.org/10.1039/C8TA03397H>
- [23] Hao, F.B., Zhang, Z.W. and Yin, L.W. (2013) $\text{Co}_3\text{O}_4/\text{Carbon Aerogel Hybrids}$ as Anode Materials for Lithium-Ion Batteries with Enhanced Electrochemical Properties. *Applied Materials & Interfaces*, **5**, 8337-8344.
<https://doi.org/10.1021/am400952j>
- [24] Wang, Q., Xiang, L.P., Mei, D. and Xie, Y.S. (2020) Graphene Aerogels: Structure Control, Thermal Characterization and Thermal Transport. *International Journal of Thermophysics*, **41**, Article No. 155.
<https://doi.org/10.1007/s10765-020-02740-6>

- [25] Guo, H.J., Sun, Q.M., Li, X.H., Wang, Z.X. and Peng, W.J. (2009) Synthesis and Electrochemical Performance of $\text{Co}_3\text{O}_4/\text{C}$ Composite Anode for Lithium Ion Batteries. *Transactions of Nonferrous Metals Society of China*, **19**, 372-376. [https://doi.org/10.1016/S1003-6326\(08\)60280-0](https://doi.org/10.1016/S1003-6326(08)60280-0)
- [26] Atomic Layer-by-Layer $\text{Co}_3\text{O}_4/\text{Graphene}$ Composite for High Performance Lithium-Ion Batteries. *Advanced Energy Materials*, **6**, Article ID: 1501835. <https://doi.org/10.1002/aenm.201501835>
- [27] Li, B.J., Cao, H.Q., Shao, J., Li, G.Q., Qu, M.Z. and Yin, G. (2011) $\text{Co}_3\text{O}_4/\text{graphene}$ Composites as Anode Materials for High-Performance Lithium Ion Batteries. *Inorganic Chemistry*, **50**, 1628-1632. <https://doi.org/10.1021/ic1023086>
- [28] Shen, J., Wang, J., Zhai, J.W., Guo, Y.Z., Wu, G.M., Zhou, B. and Ni, X.Y. (2004) Carbon Aerogel Films Synthesized at Ambient Conditions. *Journal of Sol-Gel Science and Technology*, **31**, 209-213. <https://doi.org/10.1023/B:JSST.0000047989.39431.d5>
- [29] Murray, V., Hall, D.S. and Dahn, J.R. (2019) A Guide to Full Coin Cell Making for Academic Researcher. *Journal of the Electrochemical Society*, **166**, A329-A333. <https://doi.org/10.1149/2.1171902jes>
- [30] Wang, X., Zhou, B., Guo, J., Zhang, W.P. and Guo, X.H. (2016) Selective Crystal Facets Exposing of Dumbbell-Like Co_3O_4 towards High Performances Anode Materials in Lithium-Ion Batteries. *Materials Research Bulletin*, **83**, 414-422. <https://doi.org/10.1016/j.materresbull.2016.05.028>
- [31] Binotto, G., Larcher, D., Prakash, A.S., Urbina, R.H., Hedge, M.S. and Tarascon, J.M. (2007) Synthesis, Characterization, and Li-Electrochemical Performance of Highly Porous Co_3O_4 Powders. *Chemistry of Materials*, **19**, 3032-3040. <https://doi.org/10.1021/cm070048c>
- [32] Laruelle, S., Grugeon, S., Poizot, P., Dolle, M., Dupont, L. and Tarascon, J.M. (2002) On the Origin of the Extra Electrochemical Capacity Displayed by MO/Li Cells at Low Potential. *Journal of the Electrochemical Society*, **149**, A627-A634. <https://doi.org/10.1149/1.1467947>
- [33] Li, Q., Li, H.S., Xia, Q.T., Hu, Z.Q., Zhu, Y., Yan, S.S., Ge, C., Zhang, Q.H., Wang, X.X., Shang, X.T., Fan, S.T., Long, Y.Z., Gu, L., Miao, G.X., Yu, G.H. and Moodera, J.S. (2020) Extra Storage Capacity in Transition Metal Oxide Lithium-Ion Batteries Revealed by *in Situ* Magnetometry. *Nature Materials*. <https://doi.org/10.1038/s41563-020-0756-y>
- [34] Yao, W.L., Yang, J., Wang, J.L. and Nuli, Y.N. (2008) Multilayered Cobalt Oxide Platelets for Negative Electrode Material of a Lithium-Ion Battery. *Journal of the Electrochemical Society*, **155**, A903-A908. <https://doi.org/10.1149/1.2987945>
- [35] Meddings, N., Heinrich, M., Overney, F., Lee, J.S., Ruiz, V., Napolitano, E., Seitz, S., Hinds, G., Raccichini, R., Gaberscek, M. and Park, J. (2020) Application of Electrochemical Impedance Spectroscopy to Commercial Li-Ion Cells: A Review. *Journal of Power Sources*, **480**, Article ID: 228742. <https://doi.org/10.1016/j.jpowsour.2020.228742>
- [36] Heinrich, M., Wolff, N., Harting, N., Laue, V., Roder, F., Seitz, S. and Krewer, U. (2019) Physico-Chemical Modeling of a Lithium-Ion Battery: An Ageing Study with Electrochemical Impedance Spectroscopy. *Batteries & Supercaps*, **2**, 530-540. <https://doi.org/10.1002/batt.201900011>
- [37] Zhang, S.S., Xu, K. and Jow, T.R. (2006) EIS Study on the Formation of Solid Electrolyte Interface in Li-Ion Battery. *Electrochimica Acta*, **51**, 1636-1640. <https://doi.org/10.1016/j.electacta.2005.02.137>